

Trans Effects in Nitric Oxide Binding to Myoglobin Cavity Mutant H93G[†]

Sean M. Decatur,[‡] Stefan Franzen,[§] Gia D. DePillis,[‡] R. Brian Dyer,[§] William H. Woodruff,[§] and Steven G. Boxer^{*‡}

Department of Chemistry, Stanford University, Stanford, California 94350-5080, and Biosciences and Biotechnology Group, CST-4 MS C345, Los Alamos National Laboratory, Los Alamos, New Mexico 87545

Received July 19, 1995; Revised Manuscript Received February 7, 1996[®]

ABSTRACT: When nitric oxide (NO) binds to heme proteins, it exerts a repulsive *trans* effect on the proximal ligand, resulting in weakening or rupture of the proximal ligand-iron bond. The general question of whether NO binding generates a five-coordinate complex with proximal ligand release is important for the function of enzymes such as guanylate cyclase. This question can be addressed by studying NO binding to the myoglobin cavity mutant H93G, where the proximal histidine has been replaced by glycine. When this protein is expressed in the presence of imidazole (Im), an imidazole molecule occupies the proximal cavity and serves as a ligand to the iron [Barrick, D. (1994) *Biochemistry* 33, 6546–6554]. This proximal imidazole can be exchanged for a variety of exogenous ligands [DePillis, G. D., Decatur, S. M., Barrick, D., & Boxer, S. G. (1994) *J. Am. Chem. Soc.* 116, 6981–6982]. While CO binds to H93G(Im) to form a stable six-coordinate complex similar to that of the wild type and NO binds to wild-type myoglobin to form a six-coordinate complex, we find that the binding of NO to H93G(Im) under similar conditions results in the cleavage of the exogenous imidazole–iron bond at neutral pH, leaving a five-coordinate heme–NO complex, H93G–NO, inside the protein. When a large excess of imidazole is added to this five-coordinate NO complex, a six-coordinate complex can be formed; thus, the binding constant of a sixth ligand to the five-coordinate H93G–NO complex can be measured. This is found to be several orders of magnitude smaller than the binding constant of Im to the carbonmonoxy, deoxy, or the metcyano forms of the protein. By replacement of Im with methyl-substituted imidazoles which have hindered or strained binding conformations, this binding constant can be reduced further and some of the factors responsible for favoring the five-coordinate form can be elucidated. Thus, the cavity mutant H93G provides a novel model system for studying the factors that control the coordination state of NO complexes of heme proteins and serves as a bridge between synthetic heme model complexes in simple solvents and site-directed mutants in the structured environment found in proteins.

Nitric oxide (NO)¹ has been shown to play a central role in many biological processes such as signal transduction, for example, serving as an intercellular messenger in vasodilation and neurotransmission (Gelperin, 1994; Snyder, 1992; Stamler et al., 1992). Heme proteins play important roles in both nitric-oxide generation (e.g., NO synthase, which produces NO from L-arginine) and as receptors for NO (e.g., guanylate cyclase, which catalyzes the production of cGMP from GTP during signal transduction). A key issue in these systems is whether the proximal fifth ligand to the heme iron in the resting state, often histidine, is broken upon binding of NO on the opposite (distal) side of the heme. Whereas native Mb forms a stable six-coordinate complex upon NO binding,

retaining the proximal His93–Fe bond, the ligand from the protein *trans* to NO is broken in guanylate cyclase and a number of other proteins (De Sanctis et al., 1994; Ascenzi et al., 1985, 1992; Coletta et al., 1990; Adachi et al., 1993; Morishima et al., 1989) and at low pH upon protonation of the proximal histidine in native Mb (Duprat et al., 1995). In the case of guanylate cyclase, this bond rupture may be important for initiation of a structural change which turns on enzymatic activity (Stone & Marletta, 1994; Burstyn et al., 1995; Stone et al., 1995; Yu et al., 1994).

Simple chemical models of NO and CO bonding in ferrous heme complexes have provided considerable information on the factors that control five versus six coordination. While both NO and CO are strong ligands to synthetic ferrous hemes, NO heme complexes have a large repulsive *trans* effect, such that, when NO binds to a five-coordinate ferrous heme, the bond to the axial ligand *trans* to the NO is weakened. In CO complexes, the bond of the *trans* axial ligand actually is strengthened. Furthermore, the NO–iron bond is stronger in the absence of a *trans* ligand; the opposite is true in CO complexes. Thus, NO is distinct from CO in its ability to readily form stable five-coordinate heme complexes (Wayland & Olson, 1974; Sharma & Traylor, 1992; Traylor et al., 1993). While the binding constant for imidazole to five-coordinate heme–NO has been estimated (Traylor & Sharma, 1992), this constant has not been

[†] This work is supported in part by Grant GM27738 from the National Institutes of Health to S.G.B. S.M.D. was the recipient of a NSF Predoctoral Fellowship and a Ford Foundation Dissertation Fellowship; G.D.D. was an NIH Postdoctoral Fellow.

[‡] Stanford University.

[§] Los Alamos National Laboratory.

[®] Abstract published in *Advance ACS Abstracts*, March 15, 1996.

¹ Abbreviations: NO, nitric oxide; Mb, myoglobin; CO, carbon monoxide; MbCO, carbonmonoxymyoglobin; MbNO, nitrosylmyoglobin; Im, imidazole; MeIm, methylimidazole; L, ligand; H93G(L), myoglobin cavity mutant H93G with L incorporated as a proximal ligand; H93G–NO, five-coordinate complex of NO bound to H93G Mb; H93G(L)–NO, six-coordinate complex of NO bound to H93G(L); EPR, electron paramagnetic resonance.

determined experimentally. Furthermore, it would be desirable to obtain information on the factors which govern ligand binding in the context of a protein environment where additional interactions such as hydrogen bonding may be important.

In the myoglobin cavity mutant H93G (Barrick, 1994), the functionally critical proximal histidine residue can be replaced by many exogenous organic ligands (DePillis et al., 1994). When mimics of the histidine side chain, such as imidazole (Im) or methyl-substituted imidazoles (MeIm), are introduced into the cavity, these proteins form six-coordinate ferrous CO complexes which are very similar to that of wild-type Mb, as probed by UV/vis absorption, ^1H NMR, and IR spectroscopies, as well as ligand recombination kinetics (DePillis et al., 1994; Decatur & Boxer, 1995; Decatur et al., 1996a). We have discovered that under similar conditions NO binding to these complexes results in electronic absorption spectra which are quite different from those of native MbNO. As shown in the following, these spectral changes are consistent with release of the proximal imidazole ligand and formation of a five-coordinate NO-heme, in contrast to the hexacoordinate complexes of the wild-type (WT) protein. Thus, this system provides a novel model for studying the factors that control the coordination state of heme-NO complexes and a bridge between simple synthetic heme complexes and the structured environment found in proteins.

MATERIALS AND METHODS

Protein Preparation and Purification. The sperm whale myoglobin mutant H93G was expressed and purified as described previously (Barrick, 1994; DePillis et al., 1994; Decatur & Boxer, 1995). When this mutant is expressed in *Escherichia coli* in the presence of imidazole, an imidazole molecule is incorporated into the proximal cavity and serves as a ligand to the iron (Barrick, 1994). This imidazole can be exchanged for other heterocyclic ligands using a simple diafiltration technique (DePillis et al., 1994), generating a diverse set of proteins with widely variable properties.

Preparation of the Ferrous NO Complex. Protein solutions were purged under a stream of N_2 gas in a vial or cuvette sealed with a rubber septum. A minimal amount of sodium dithionite was added to the samples from a freshly prepared 1 M stock solution. The protein solution was then placed under a stream of NO gas to produce the NO complex.

EPR Spectroscopy. X-band EPR spectra were measured at 77 K on a Varian E112 EPR spectrometer equipped with a quartz dewar. Samples were ~ 1 mM protein in 60% glycerol/water and 100 mM phosphate (pH = 7.0).

NO Dissociation Rates. The rate of dissociation of NO from Mb was measured using the CO replacement technique (Moore & Gibson, 1976; Sharma & Ranney, 1978). Three milliliters of buffer (100 mM phosphate, pH = 7.0) was added to a quartz cuvette, sealed with a septum, purged with N_2 , and then equilibrated with CO. Freshly prepared sodium dithionite solution was added to a total concentration of 1 mM. A concentrated stock solution of MbNO was prepared by addition of 1 atm of NO to a sealed vial of concentrated deoxymyoglobin (~ 1 mM). An aliquot of the MbNO solution was added to the cuvette to give a Soret band absorbance of ~ 1 . The UV/vis absorption spectra were then measured every 30 s for ~ 3 h.

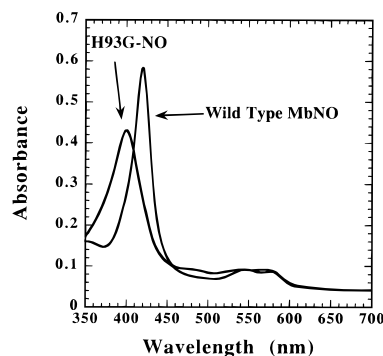


FIGURE 1: Absorption spectra of wild-type MbNO ($\lambda_{\text{max}} = 421$ nm) and H93G-NO ($\lambda_{\text{max}} = 400$ nm). The samples were in 100 mM phosphate (pH = 7.0); the H93G sample contained 10 μM excess imidazole.

Resonance Raman Spectra. Resonance Raman spectra were obtained with an Ar ion laser (Coherent Innova 400) pumping a dye laser (Coherent CR-559) using the laser dye Stilbene 420 to excite the sample at 423 nm. The dye laser output was spectrally filtered using a grating and pinhole apparatus to remove small satellite laser lines. Spectra were obtained using a 135° back-scattering geometry. The scattered light was collected and analyzed with a Photometrics CCD detector. Spectral slit widths were set for a resolution of 2.4 cm^{-1} . Sample concentrations ranged from 50 to 100 μM for WT MbNO and from 100 to 300 μM for H93G-NO.

RESULTS

Coordination State of H93G-NO. The electronic absorption spectra of WT MbNO and H93G-NO, prepared by dilution of a concentrated stock of H93G-NO into 100 mM phosphate buffer (pH = 7.0), are compared in Figure 1. The Soret band of H93G-NO is broad and blue-shifted by ~ 22 nm relative to that of WT MbNO. Its spectrum is similar to that of five-coordinate NO-heme complexes, which also exhibit broadened, blue-shifted Soret bands (Coletta et al., 1990). Identical absorption spectra are observed when NO binds to H93G(L), where L = methylimidazoles or pyridine, and in the NO complexes of the human myoglobin mutants H93C and H93Y (Adachi et al., 1993).

Ferrous MbNO is a low-spin paramagnetic complex with $S = 1/2$, and the hyperfine splitting observed in the low-temperature EPR spectrum is indicative of the coordination state of the heme iron (Stone et al., 1995; Mun et al., 1979; Hille et al., 1979). In WT MbNO at pH = 6.5, hyperfine splitting from ^{14}NO and ^{14}N of the proximal histidine results in a poorly resolved nine-line pattern, a signature of the six-coordinate complex (Figure 2A). By contrast, the EPR spectrum of H93G-NO at pH = 6.5 (Figure 2B) exhibits the three-line pattern characteristic of the five-coordinate heme-NO complex and quite similar to the spectrum reported recently for guanylate cyclase upon NO binding (Stone et al., 1995).

Resonance Raman spectroscopy is also a useful probe of the coordination state of the heme iron. In the six-coordinate complex, the iron lies almost in the plane of the heme, while in the five-coordinate species, the iron is displaced from the heme plane toward the NO ligand (Scheidt & Frisse, 1975; Scheidt & Piculo, 1976; Scheidt et al., 1977). The core-size marker modes of the heme are sensitive to the position of the iron and are therefore sensitive to its oxidation and

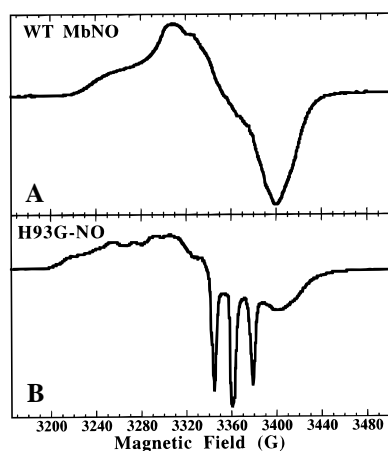


FIGURE 2: X-band EPR spectra at 77 K of (A) wild-type MbNO and (B) H93G-NO. In both samples, [Mb] \sim 1 mM and pH = 6.5. For H93G-NO, the [Im] in solution was \sim 1 mM.

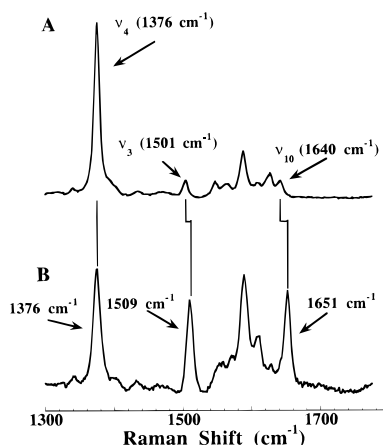


FIGURE 3: High-frequency region of the resonance Raman spectra of (A) wild-type MbNO and (B) H93G-NO. Spectra were recorded at room temperature in 0.1 M phosphate buffer (pH = 7.0). The concentration of H93G was \sim 100 μ M with \sim 30 μ M excess Im present in solution. Frequencies are compared to known frequencies of five- and six-coordinate heme-NO complexes in Table 1.

Table 1: Comparison of Core-Size Marker Modes in Five- and Six-Coordinate Heme-NO Compounds

	ν_3	ν_{10}
five-coordinate complexes		
H93G-NO	1509	1651
iron(II) protoporphyrin IX-NO ^a	1508	1648
guanylate cyclase ^b	1508	1646
six-coordinate complexes		
MbNO ^a	1501	1638
HbNO ^a	1500	1636

^a Tsubaki and Yu (1982). ^b Yu et al. (1994).

coordination states (Spiro & Li, 1988). Five-coordinate heme-NO complexes can be distinguished by small shifts in the ν_3 and ν_{10} modes relative to those of six-coordinate heme-NO, increased intensity in the ν_{10} mode, and decreased intensity in the ν_4 oxidation state marker mode (Yu et al., 1994; Yu & Kerr, 1988; Benko & Yu, 1983). The resonance Raman spectra of the core-size marker region in WT MbNO and H93G-NO are presented in Figure 3; the data are summarized and compared to literature values in Table 1. Significantly, the frequencies of these modes in H93G-NO are similar to those observed in NO-bound guanylate cyclase (Yu et al., 1994) and five-coordinate heme model compounds.

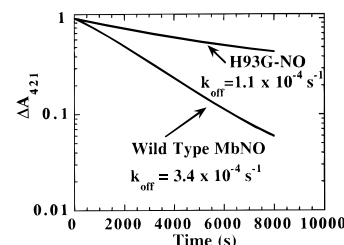


FIGURE 4: k_{off} measurements for H93G-NO and wild type MbNO. Samples were prepared as described in Materials and Methods. [Mb] in both samples was \sim 2 μ M; the H93G-NO sample contained $<$ 10 μ M Im in solution.

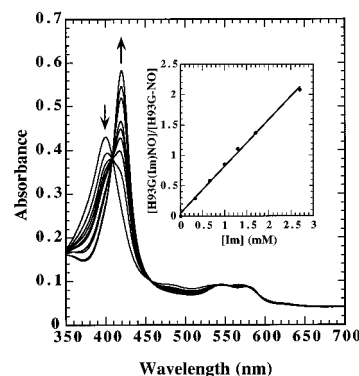


FIGURE 5: Titration of H93G-NO with imidazole. The concentration of H93G was \sim 2 μ M in 0.1 M phosphate buffer (pH = 7.0) at 295 K. The inset is a plot of [Im] versus [H93G(Im)NO]/[H93G-NO]. The slope of this plot gives K , according to eqs 1 and 2. Im concentrations were corrected for the fraction of protonated imidazole (ImH⁺) present at pH 7.

NO Dissociation Rates. The dissociation rates for NO in WT MbNO and H93G-NO complexes were measured by the CO replacement technique; the change in absorbance (cf. Figure 2) at 421 nm (WT) or 400 nm (H93G) follows the disappearance of MbNO (Figure 4). The kinetics for both WT and H93G-NO can be fit well by a single exponential. The rate constant for H93G ($k_{\text{off}} = 1.1 \times 10^{-4} \text{ s}^{-1}$) is 3-fold smaller than that of WT ($k_{\text{off}} = 3.4 \times 10^{-4} \text{ s}^{-1}$). The slower dissociation rate in H93G might reflect the presence of a higher binding constant for NO in a five-coordinate complex (Traylor & Sharma, 1992).

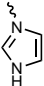
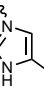
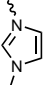
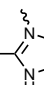
Equilibrium between Five- and Six-Coordinate Forms. The six-coordinate complex H93G(Im)NO is formed when a high concentration of Im is present in solutions of H93G-NO. The transition from the five- to six-coordinate complex can be readily observed in the visible absorption spectrum as shown in Figure 5. Upon addition of excess imidazole, the Soret band maximum shifts from 400 to 420 nm, with an isobestic point at 408 nm. The observed spectral changes occur immediately upon addition of Im, much faster than the observed NO dissociation rates shown in Figure 4. These spectral changes can be used to calculate an equilibrium constant for the binding of Im to H93G-NO.



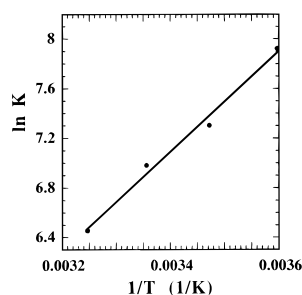
$$K = \frac{[\text{H93G(Im)NO}]}{[\text{H93G-NO}][\text{Im}]} \quad (2)$$

Absorbance spectra were measured over a range of Im concentrations, and the [H93G(Im)NO]/[H93G-NO] ratio was determined. A plot of [H93G(Im)NO]/[H93G-NO] versus [Im] gives a line with slope K [Figure 5, inset; Im

Table 2: K and ΔG° for Binding Different Exogenous Ligands to the Five-Coordinate H93G–NO Complex at 295 K^a

ligand ^a	K	ΔG° (kJ/mol)
imidazole 	$(1.5 \pm 0.1) \times 10^3$	–18
4-methylimidazole 	$(2.0 \pm 0.1) \times 10^3$	–19
<i>N</i> -methylimidazole 	$(0.7 \pm 0.04) \times 10^3$	–16
2-methylimidazole 	$(0.025 \pm 0.005) \times 10^3$	–7

^a cf. eqs 1 and 2.

FIGURE 6: van't Hoff plot of the binding constant of Im to H93G–NO. On the basis of a least squares fit, $\Delta H^\circ = -34$ kJ/mol and $\Delta S^\circ = -55$ J/mol.

concentrations were corrected for the fraction of protonated imidazole (ImH^+) present at pH = 7]. K and ΔG° for imidazole and several other exogenous ligands are listed in Table 2. The K for 4-MeIm is slightly larger than that for Im, while *N*-MeIm has a smaller binding constant. This order of binding preference is the same as that observed in the metcyano complexes of H93G (Decatur & Boxer, 1995; Decatur, 1995). The binding constant of Im to H93G–NO was measured over the temperature range 5–35 °C. A van't Hoff plot of $\ln K$ versus $1/T$ is given in Figure 6; the significant temperature dependence of K reflects a large enthalpic term ($\Delta H^\circ \sim -33$ kJ/mol) and a relatively small entropic contribution [$\Delta S^\circ \sim -55$ J/(mol K)].

DISCUSSION

Binding of NO to H93G(Im) Promotes Im Dissociation. As shown by absorption, EPR, and resonance Raman spectra, the Mb mutant H93G(Im) forms a five-coordinate heme–NO complex, H93G–NO, displacing the proximal exogenous Im, unless a large excess concentration of Im is present. Anticipating this conclusion, we have used H93G–NO to denote the five-coordinate species and H93G(Im)NO to denote the six-coordinate species. Thus, as with model heme–NO complexes, the Im–iron bond in H93G(Im) is weakened by the binding of NO. This contrasts with the wild-type protein, in which NO binding does not displace the proximal His93 and the carbonmonoxy- and deoxy- forms

of H93G(Im), in which the Im remains bonded to the iron (DePillis et al., 1994; Franzen et al., 1995; Decatur et al., 1996).

Contributions to the Imidazole Binding to H93G–NO. The lack of a covalent bond between the Im ligand and the polypeptide chain in H93G enables the measurement of a binding constant and free energy for the proximal ligand to H93G–NO via a simple titration. There are several factors which can contribute to the binding energy of imidazole to H93G–NO, including the energy of the covalent bond with the iron, noncovalent interactions with the protein (such as hydrogen bonds or van der Waals contacts), and entropic contributions from both the displacement of water from the binding cavity and the sequestration of the ligand from the aqueous solution. The temperature dependence of the equilibrium constant suggests that ΔG° is dominated by a large negative enthalpic term. The important factors in stabilization of the Im in the proximal cavity are likely the covalent bond between the Im and the heme iron and noncovalent bonding interactions between the Im and the proximal cavity. The data presented here can not quantitatively further separate these different contributions. For example, we do not know whether Im occupies the proximal cavity even when not bonded to the iron (a state analogous to geminate binding for diatomic ligands on the distal side). The identification of such an intermediate would permit the direct measurement of Im bonding to heme independent of Im binding to the protein cavity.

We have shown elsewhere that methyl-substituted imidazoles bind to the metcyano complex of H93G with unique affinities and conformations, depending on the interactions between the ligand and the amino acids of the protein cavity (Decatur & Boxer, 1995; Decatur et al., 1996b; Decatur, 1995). According to the measured binding affinities listed in Table 2, the series of methyl-substituted imidazoles bind with decreasing affinity in the order 4-MeIm \sim Im $>$ *N*-MeIm \gg 2-MeIm. The same trend is observed in the carbonmonoxy complex (Decatur et al., 1996b) and in the deoxy form (Franzen, Decatur, and Boxer, to be published). 4-MeIm forms a slightly more stable six-coordinate complex than Im; this observation is consistent with the fact that 4-MeIm has a higher pK_a than Im and is a better electron donor, producing a stronger ligand–metal bond. *N*-MeIm, however, has a significantly weaker binding than Im or 4-MeIm, although in free solution, the pK_a of *N*-MeIm is similar to that of 4-MeIm. Unlike Im or 4-MeIm, *N*-MeIm is not capable of hydrogen bonding with potential hydrogen bond acceptors such as Ser92 or the backbone carbonyl of Leu89. The lack of a hydrogen bond can affect *N*-MeIm binding in two different mechanisms. As suggested by NMR spectroscopy, there are modest differences in conformation between 4-MeIm and *N*-MeIm in the metcyano complex of H93G (Decatur & Boxer, 1995), and this change in conformation and the absence of a hydrogen bond to Ser92 may combine to destabilize *N*-MeIm binding. Alternatively, donation of a hydrogen bond by 4-MeIm increases its effective pK_a . Therefore, while 4-MeIm and *N*-MeIm may have comparable basicities in free solution, the presence or absence of a hydrogen bond can modulate the basicity of the proximal imidazole and therefore the strength of the iron–imidazole bond (Decatur et al., 1996b). 2-MeIm binds about 2 orders of magnitude more weakly than Im; this is likely due to unfavorable steric interactions between the 2-Me

group and the heme plane. Thus, removal of a hydrogen bond or introduction of steric strain in the proximal ligand binding can greatly destabilize the formation of a six-coordinate complex. This suggests an obvious series of experiments involving further site-directed changes on the proximal side, which are in progress.

Relevance to NO Binding in Heme Proteins. The binding of substituted imidazoles to H93G–NO provides interesting insight into NO binding to other heme proteins. Direct comparisons between the binding constants for a sixth ligand to H93G–NO and the effects of NO binding on native heme proteins are not possible because the proximal ligands are covalently bound in the native proteins. Nonetheless, these studies of H93G–NO provide some information on factors which can stabilize the six-coordinate species. In other heme proteins, such as wild-type myoglobin and guanylate cyclase, the covalent attachment of the proximal histidine to the polypeptide backbone imposes constraints favoring the formation of either six- or five-coordinate NO complexes. Constraints and strain imposed upon the proximal histidine can either stabilize the iron–histidine bond or facilitate its release upon binding of NO. In the six-coordinate limit, such as in wild-type MbNO, either there is little strain in the conformation of the proximal histidine or there is no flexibility for the histidine to be displaced from its position as the ligand to the iron, and therefore, the residue remains coordinated to the iron. In the five-coordinate limit, such as NO bound to the α chains of T-state hemoglobin and to guanylate cyclase, the histidine appears to be strained from its lowest-energy conformation when bonded to the iron, and this strain energy is released when the iron–histidine bond is broken. This released strain energy in guanylate cyclase may be responsible for the conformational transition associated with NO activation.

There are significant structural differences in the binding conformation of Im in H93G(Im) as compared with histidine 93 in the wild type, at least in the metaquo form of H93G(Im) whose X-ray structure is available (Barrick, 1994). The most striking difference is a rotation of the plane of the proximal imidazole ring, characterized by the angle Φ between the projection of the Im ring onto the heme plane and the axis of the N_{II} – N_{IV} pyrrolic nitrogens. In wild-type myoglobin, $\Phi \sim 5^\circ$, while in H93G(Im), the projection of the imidazole plane nearly eclipses the α – δ meso protons to give a $\Phi \sim 40^\circ$ (Barrick, 1994). The tilt of the plane of the imidazole away from the heme normal is also larger in H93G(Im) than in wild-type sperm whale Mb, apparently due to interaction with His97, which moves considerably inward toward the proximal ligand in metaquo H93G(Im) compared with the wild type, and Leu89. These structural changes can have important implications for imidazole–heme bonding. On the basis of *ab initio* calculations, Scheidt and Chipman have postulated that the imidazole conformation found in wild-type myoglobin maximizes π bonding between the Im and the heme (Scheidt & Chipman, 1986). Thus, the difference in Φ could account for the tendency of wild-type Mb to remain six-coordinate in the ferrous NO form. However, in hemoglobin, both α and β chains of hemoglobin have $\Phi \sim 20^\circ$ (Fermi et al., 1984), but only the α chains form five-coordinate NO complexes in the T state. There is less information on the effects of tilting the Im plane away from the heme normal, though a similar tilt is observed for the histidine ligands in the R state of Hb. Because we

do not yet have a high-resolution structure of H93G(L)CO or H93G(L)NO at a high ligand concentration, it is premature to speculate further on structure-based changes in electronic properties.

The observation that the binding constant for proximal ligands L to H93G–NO varies with its chemical and structural properties demonstrates a tremendous sensitivity of proximal ligand binding in six-coordinate heme–NO to environmental factors within the protein. Thus, in a native protein, the conformation of the proximal ligand as constrained by its covalent linkage to the polypeptide chain and its interactions with the surrounding protein environment will determine whether the bond to iron is broken or maintained upon binding of NO. Thus, H93G(L) can provide a bridge between traditional model systems involving synthetic heme complexes and proteins which are only poorly understood such as guanylate cyclase. It will also be most interesting to apply the cavity mutant strategy to guanylate cyclase itself to further understand these interactions in their native context.

REFERENCES

- Adachi, S., Nagano, S., Ishimori, K., Watanabe, Y., & Morishima, I. (1993) *Biochemistry* 32, 241–252.
- Ascenzi, P., Coletta, M., Desideri, A., & Brunori, M. (1985) *Biochim. Biophys. Acta* 829, 299–302.
- Ascenzi, P., Coletta, M., Desideri, A., Petruzzelli, R., Polizio, F., Bolognesi, M., Condo, S. G., & Giardina, B. (1992) *J. Inorg. Biochem.* 45, 31–37.
- Barrick, D. (1994) *Biochemistry* 33, 6546–6554.
- Benko, B., & Yu, N.-T. (1983) *Proc. Natl. Acad. Sci. U.S.A.* 80, 7042–7046.
- Burstyn, J. N., Yu, A. E., Dierks, E. A., Hawkins, B. K., & Dawson, J. H. (1995) *Biochemistry* 34, 5896–5903.
- Coletta, M., Boffi, A., Ascenzi, P., Brunori, M., & Chiancone, E. (1990) *J. Biol. Chem.* 265, 4828–4830.
- Decatur, S. M. (1995) Ph.D. Thesis, Stanford University, Stanford, CA.
- Decatur, S. M., & Boxer, S. G. (1995) *Biochemistry* 34, 2122–2129.
- Decatur, S. M., DePillis, G. D., & Boxer, S. G. (1996a) Modulation of Protein Function by Introducing Molecules into Protein Cavities: Introduction of Exogenous Ligands in Myoglobin Cavity Mutant H93G Modulates CO Binding Properties, *Biochemistry* 35, 3925–3932.
- Decatur, S. M., Rickert, P. K., Franzen, S., & Boxer, S. G. (1996b) ^1H NMR Characterization of Myoglobins Where Exogenous Imidazoles Replace the Proximal Histidine. II. Interactions Between Imidazoles and Residue 92, *Biochemistry* (submitted for publication).
- DePillis, G. D., Decatur, S. M., Barrick, D., & Boxer, S. G. (1994) *J. Am. Chem. Soc.* 116, 6981–6982.
- De Sanctis, G., Falcioni, G., Polizio, F., Desideri, A., Giardina, B., Ascoli, F., & Brunori, M. (1994) *Biochim. Biophys. Acta* 1204, 28–32.
- Duprat, A. G., Traylor, T. G., Wu, G.-Z., Coletta, M., Sharma, V. S., Walda, K. N., & Magde, D. (1995) *Biochemistry* 34, 2634–2644.
- Franzen, S., Bohn, B., Poyart, C., DePillis, G. D., Boxer, S. G., & Martin, J.-L. (1995) *J. Biol. Chem.* 270, 1718–1720.
- Galla, H.-J. (1993) *Angew. Chem., Int. Ed. Engl.* 32, 378–380.
- Hille, R., Olson, J. S., & Palmer, G. (1979) *J. Biol. Chem.* 254, 12110–12120.
- Moore, E. G., & Gibson, Q. H. (1976) *J. Biol. Chem.* 251, 2788–2794.
- Morishima, I., Shiro, Y., Adachi, S., Yano, Y., & Oori, Y. (1989) *Biochemistry* 28, 7582–7586.
- Mun, S. K., Chang, J. C., & Das, T. P. (1979) *Proc. Natl. Acad. Sci. U.S.A.* 76, 4842–4846.
- Nagai, K., Welborn, C., Dolphin, D., & Kitagawa, T. (1980) *Biochemistry* 19, 4755–4761.

- Perutz, M. F., Kilmartin, J. V., Nagai, K., Szabo, A., & Simon, S. R. (1976) *Biochemistry* 15, 378–387.
- Scheidt, W. R., & Frisse, M. E. (1975) *J. Am. Chem. Soc.* 97, 17.
- Scheidt, W. R., & Piculo, P. L. (1976) *J. Am. Chem. Soc.* 98, 1913.
- Scheidt, W. R., & Chipman, D. M. (1986) *J. Am. Chem. Soc.* 108, 1163–1167.
- Scheidt, W. R., Brinegar, A. C., Ferro, E. B., & Kirner, J. F. (1977) *J. Am. Chem. Soc.* 99, 7315–7322.
- Sharma, V. S., & Ranney, H. M. (1978) *J. Biol. Chem.* 253, 6467–6472.
- Snyder, S. H. (1992) *Science* 257, 494–496.
- Spiro, T. G., & Li, X.-Y. (1989) in *Biological Applications of Raman Spectroscopy* (Spiro, T. G., Ed.) Vol. 3, pp 1–37, John Wiley & Sons, New York.
- Stone, J. R., & Marletta, M. A. (1994) *Biochemistry* 33, 5636–5640.
- Stone, J. R., Sands, R. H., Dunham, W. R., & Marletta, M. A. (1995) *Biochem. Biophys. Res. Commun.* 207, 372–377.
- Traylor, T. G., & Sharma, V. S. (1992) *Biochemistry* 31, 2847–2849.
- Traylor, T. G., Duprat, A. F., & Sharma, V. S. (1993) *J. Am. Chem. Soc.* 115, 810–811.
- Yu, A. E., Hu, S., Spiro, T. G., & Burstyn, J. N. (1994) *J. Am. Chem. Soc.* 116, 4117–4118.
- Yu, N.-T., & Tsubaki, M. (1982) *Biochemistry* 21, 1140–1144.
- Yu, N.-T., & Kerr, E. A. (1989) in *Biological Applications of Raman Spectroscopy* (Spiro, T. G., Ed.) Vol. 3, pp 39–95, John Wiley & Sons, New York.

BI951661P